Supplementary Information

Formulation and evaluation of microemulgel containing a non-steroidal anti-inflammatory drug

Mamatha H S*[a], Sowmya N[b], Ashok Kumar B S[c] & Disha N S[d]

[a] Department of Pharmaceutics, Faculty of Pharmacy, R. L. Jalappa College of Pharmacy, Sri Devaraj Urs Academy of Higher Education And Research, Tamaka, Kolar 563 103, Karnataka, India

[b] Department of Pharmaceutics, Faculty of Pharmacy, Vaasudhara College of Pharmacy, Hosakote 562 114, Karnataka, India

[c] Department of Pharmacognosy, Faculty of Pharmacy, R. L. Jalappa College of Pharmacy, Sri Devaraj Urs Academy of Higher Education And Research, Tamaka, Kolar 563 103, Karnataka, India

[d] Department of Pharmaceutical Chemistry, Faculty of Pharmacy, R. L. Jalappa College of Pharmacy, Sri Devaraj Urs Academy of Higher Education And Research, Tamaka, Kolar 563 103, Karnataka, India

E-mail: shreemamatha6@gmail.com

Received 27 November 2024; accepted (revised) 1 July 2025

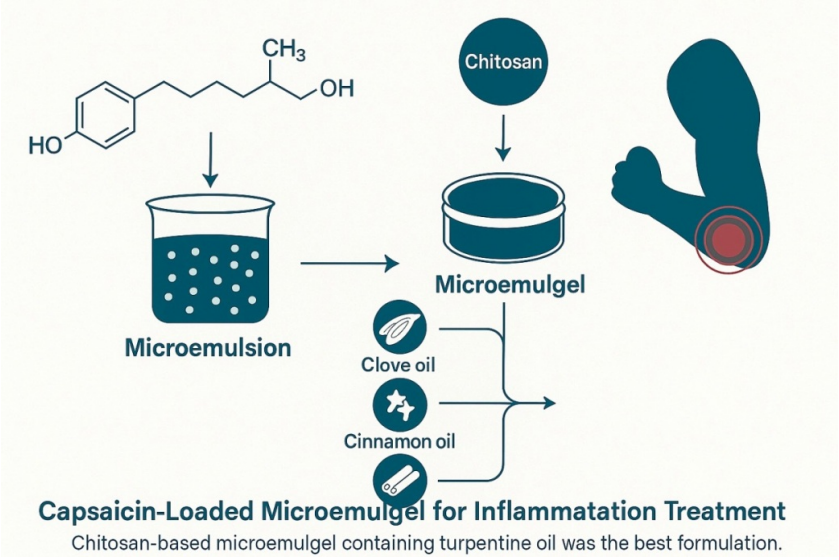

Fig. S1 — Schematic representation for Capsaicin-Loaded Microemulgel preparation for Inflammation Treatment

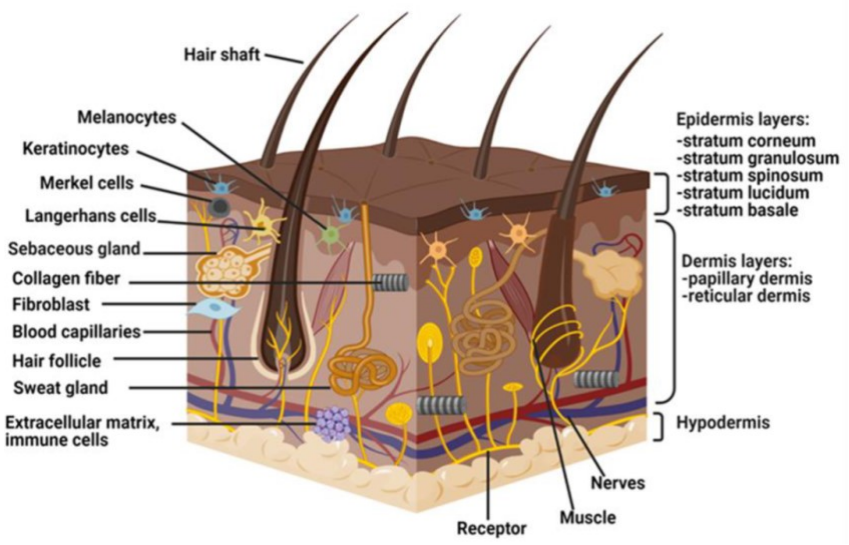

Fig. S2 — Cross-sectional structure of human skin showing layers: epidermis (with stratum corneum, granulosum, spinosum, basale), dermis, and hypodermis, each with unique drug permeation properties

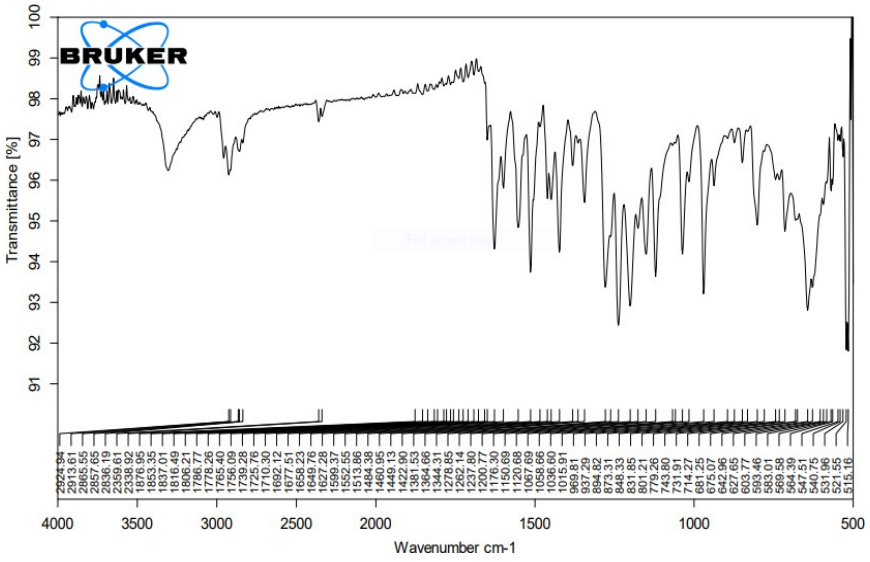

Fig. S3 — FTIR spectrum of pure capsaicin displaying major functional group peaks.

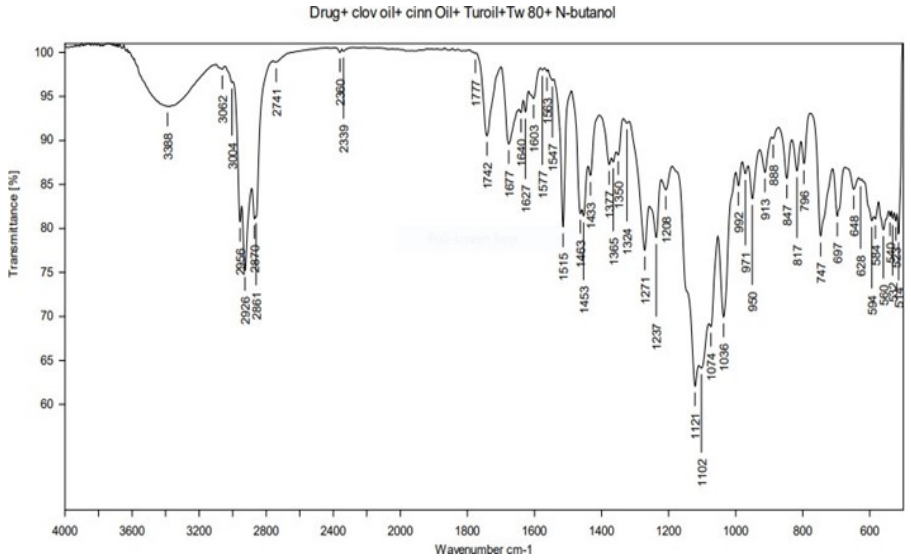

Fig. S4 — FTIR spectrum of capsaicin combined with surfactants and oils indicating absence of peak shifts.

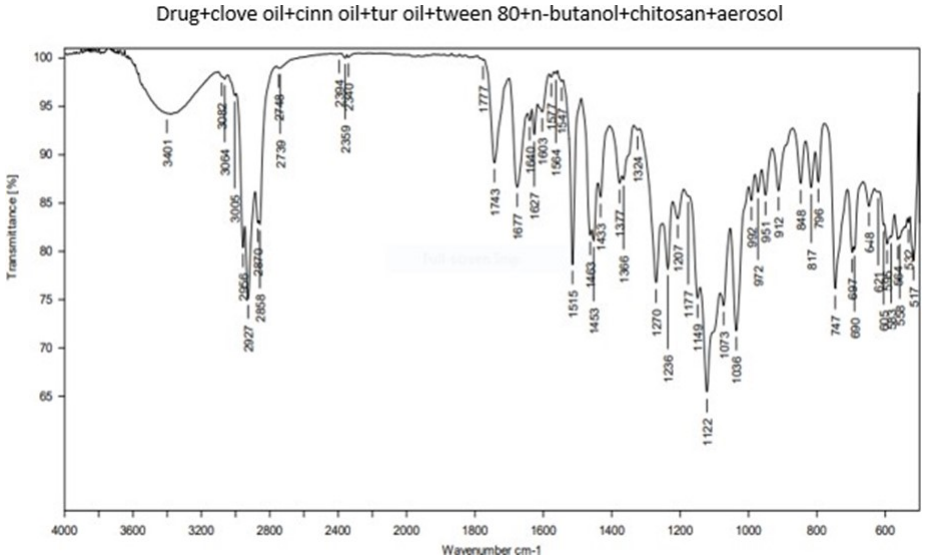

Fig. S5 — FTIR spectrum of capsaicin combined with surfactants, oils, and gelling agents showing compatibility.

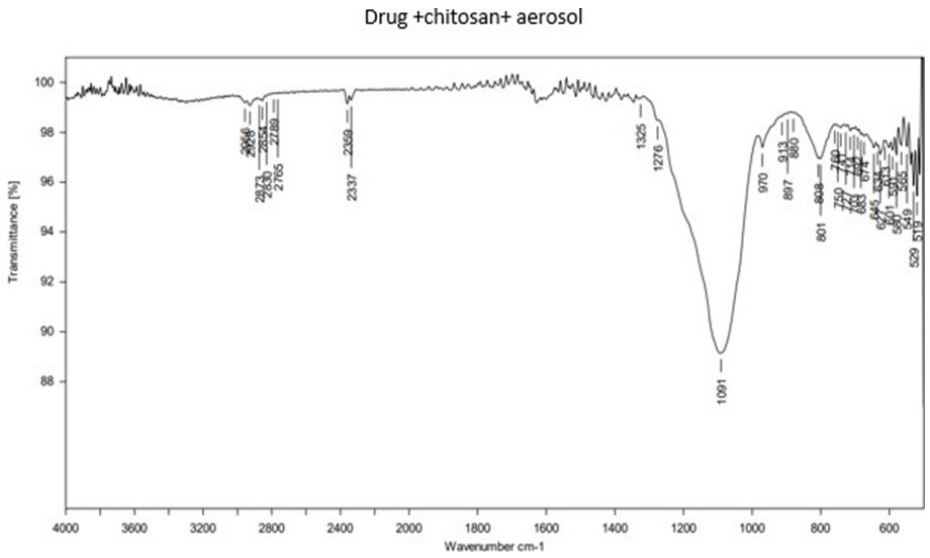

Fig. S6 — FTIR spectrum of capsaicin with gelling agents showing consistent characteristic peaks.

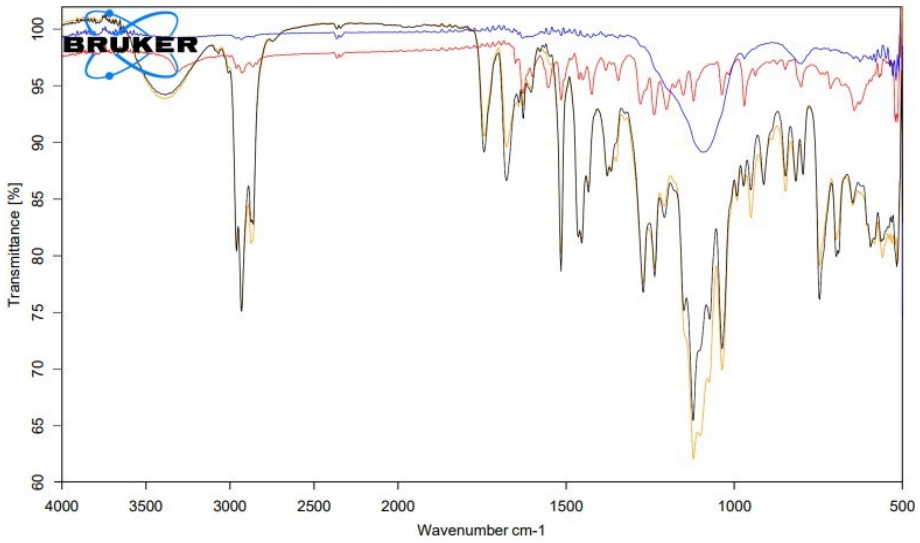

Fig. S7 — Overlay comparison of FTIR spectra of pure drug and excipient mixtures confirming no significant interactions.

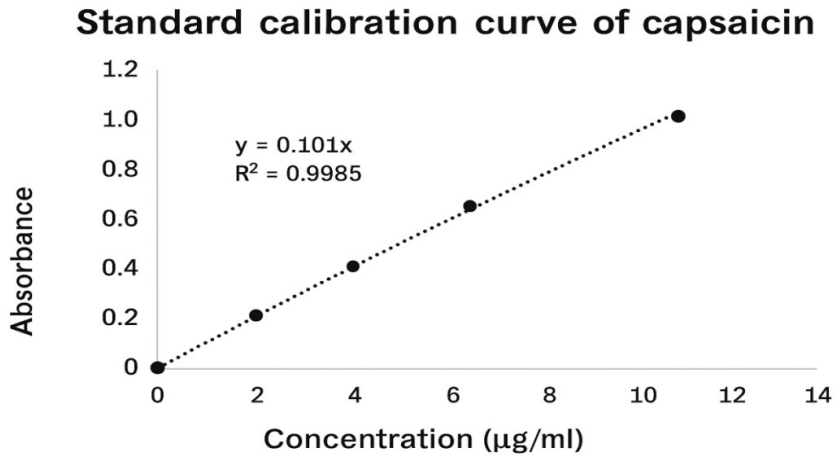

Fig. S8 — Calibration curve of capsaicin in phosphate buffer:methanol (70:30) showing linearity (R^2 = 0.9985) at λmax 280.6 nm.

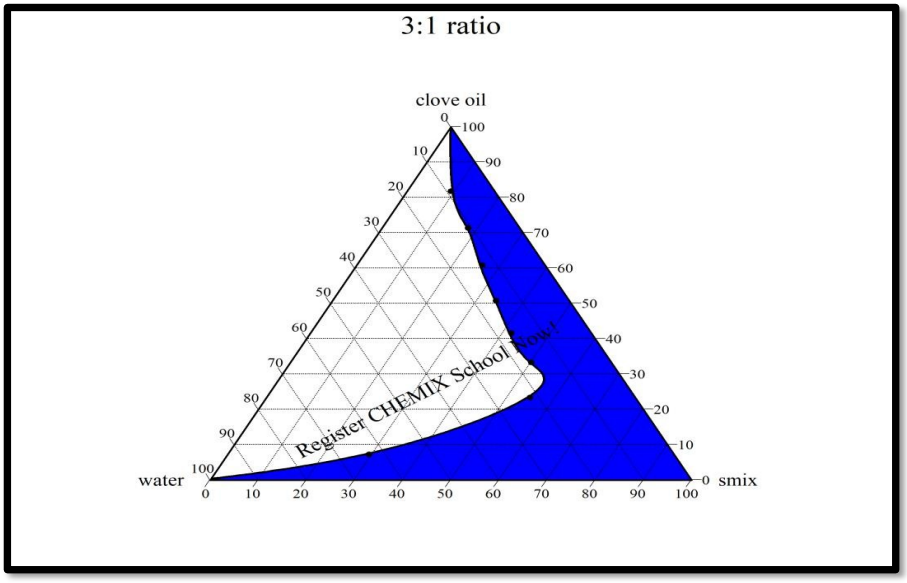

Fig. S9 — Pseudo-ternary plot diagram using clove oil as oil phase and Tween 80:n-butanol (3:1) as Smix.

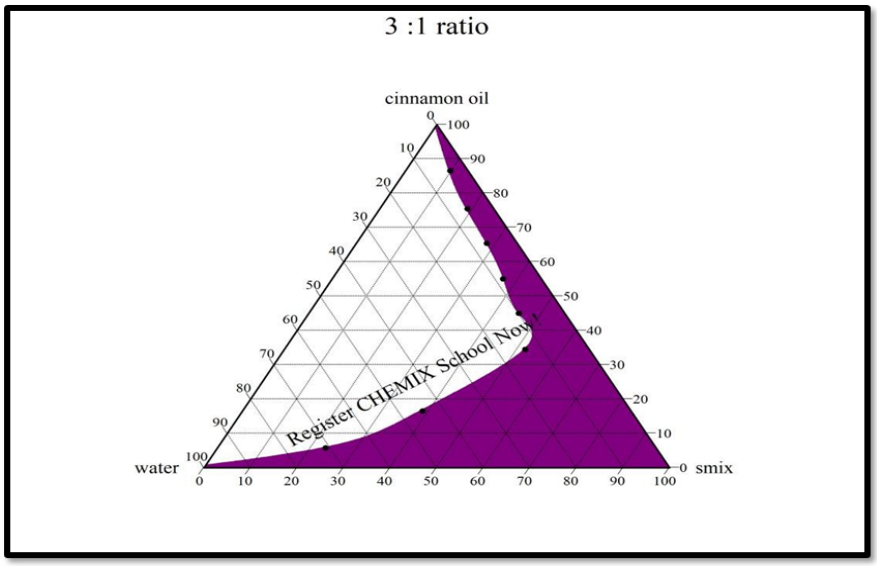

Fig. S10 — Pseudo-ternary plot using cinnamon oil as oil phase and Tween 80:n-butanol (3:1) as Smix.

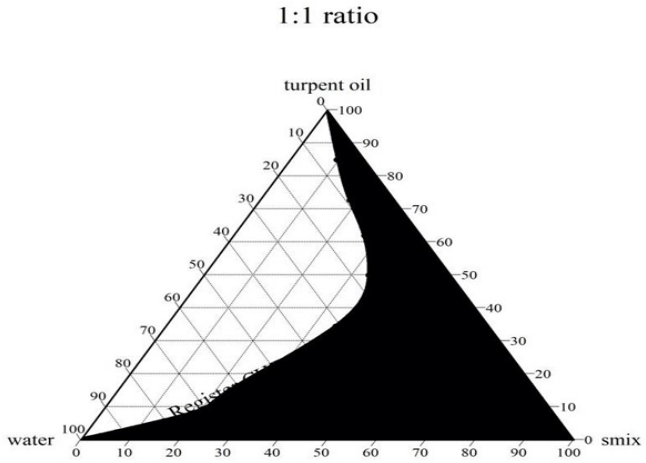

Fig. S11 — Pseudo-ternary plot with turpentine oil and Tween 80:n-butanol (1:1), showing widest microemulsion region.

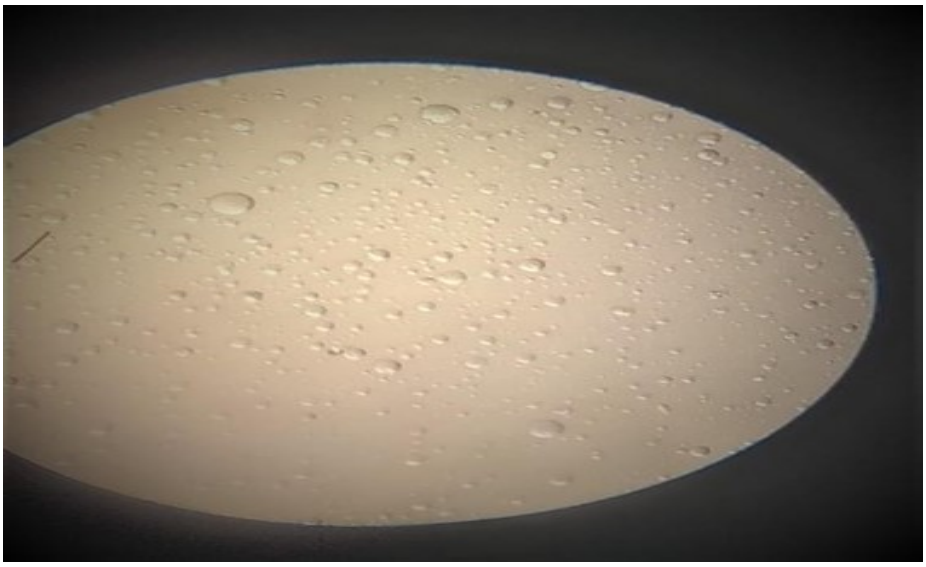

Fig. S12 — Photomicrograph of microemulsion formulation F3 showing spherical droplets and uniform dispersion.

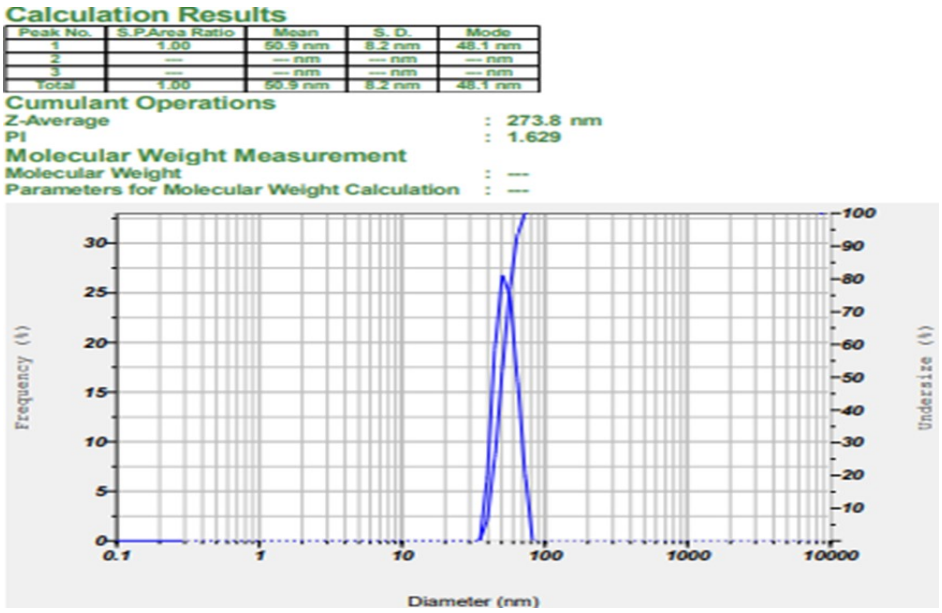

Fig. S13 — Particle size distribution and PDI of formulation F1.

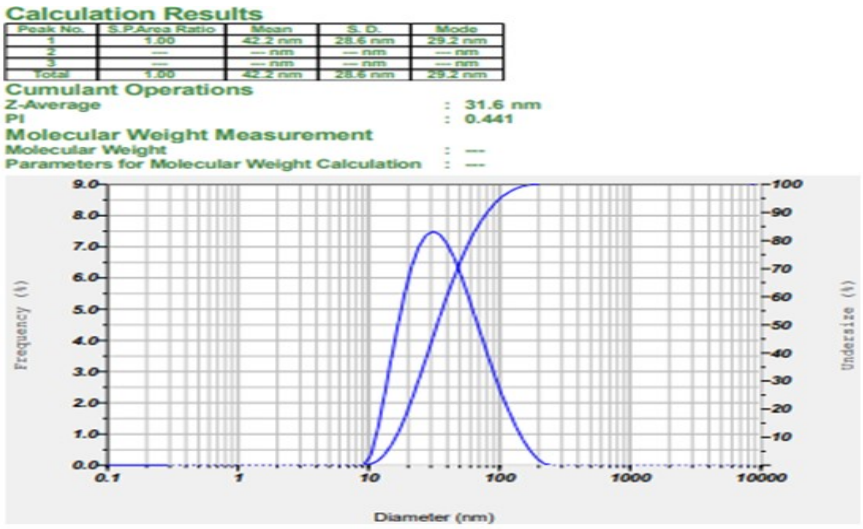

Fig. S14 — Particle size distribution and PDI of formulation F3, confirming nano-range particle size.

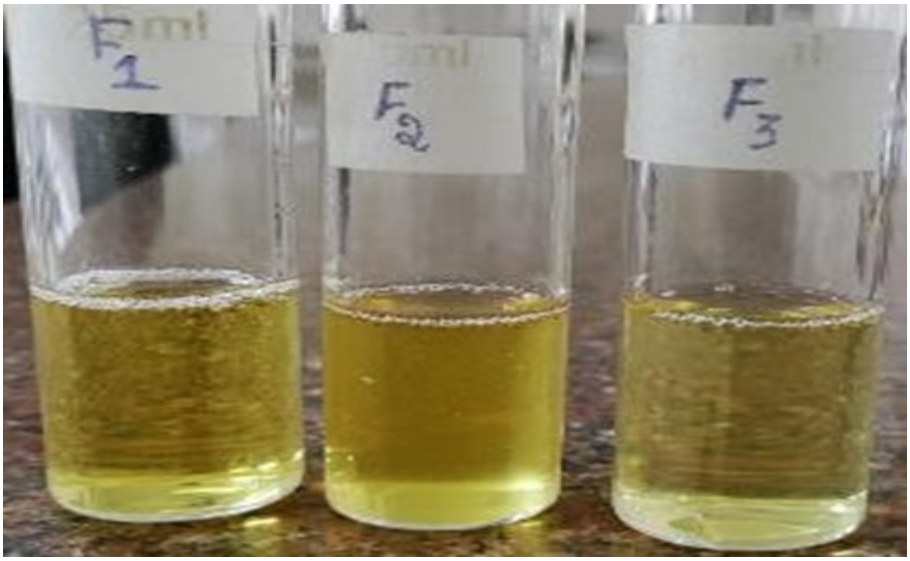

Fig. S15 — Photograph of F3 microemulsion post centrifugation indicating physical stability and no phase separation.

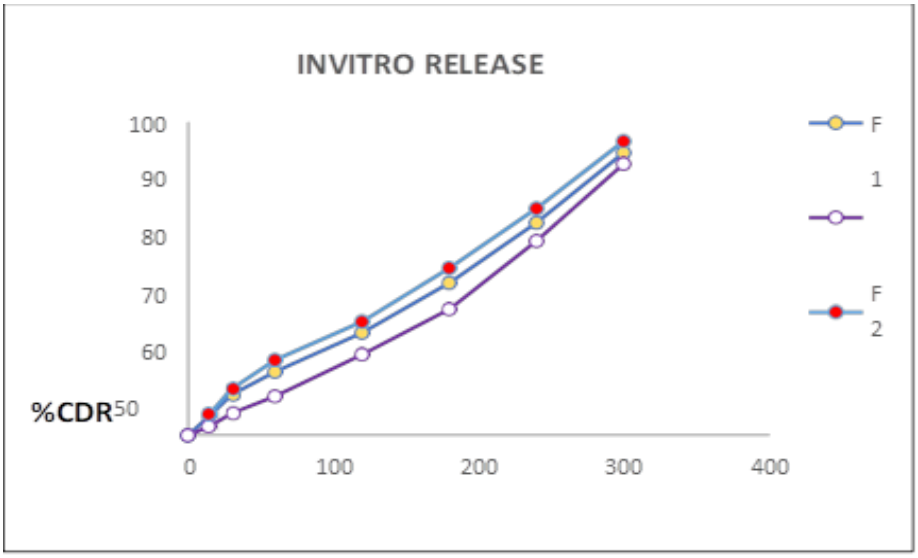

Fig. S16 — In vitro drug release profile of microemulsions F1, F2, and F3

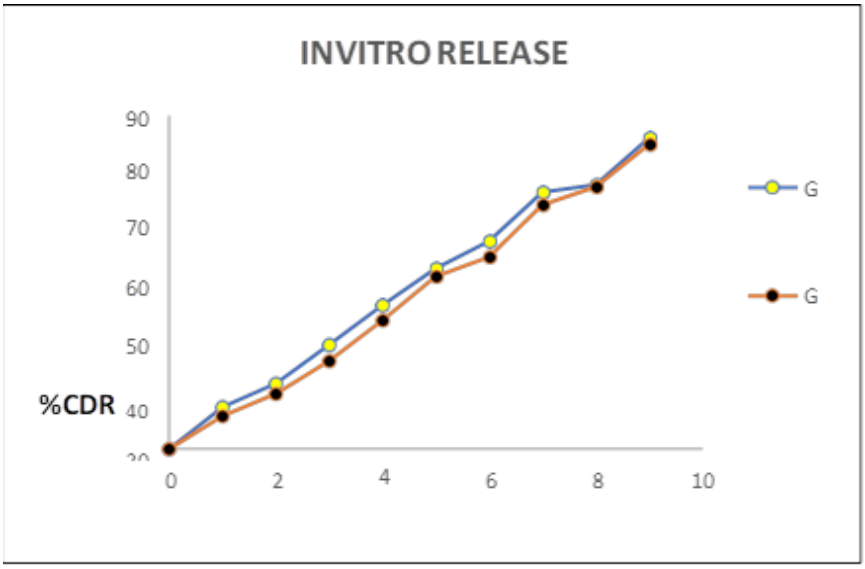

Fig. S17 — In vitro release profile of microemulgel formulations G1 and G2, demonstrating superior release from G1.

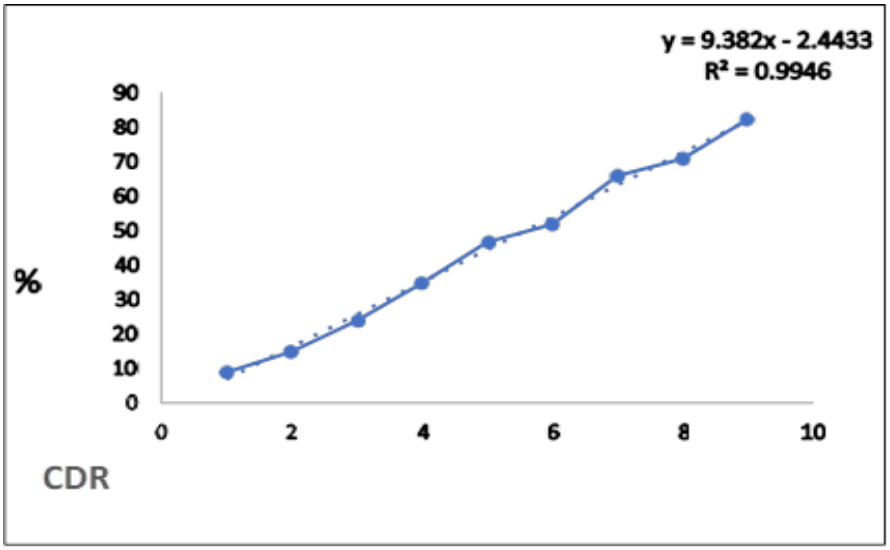

Fig. S18 — Zero-order release kinetics of capsaicin microemulgel G1 indicating controlled release ($R^2 = 0.9942$).

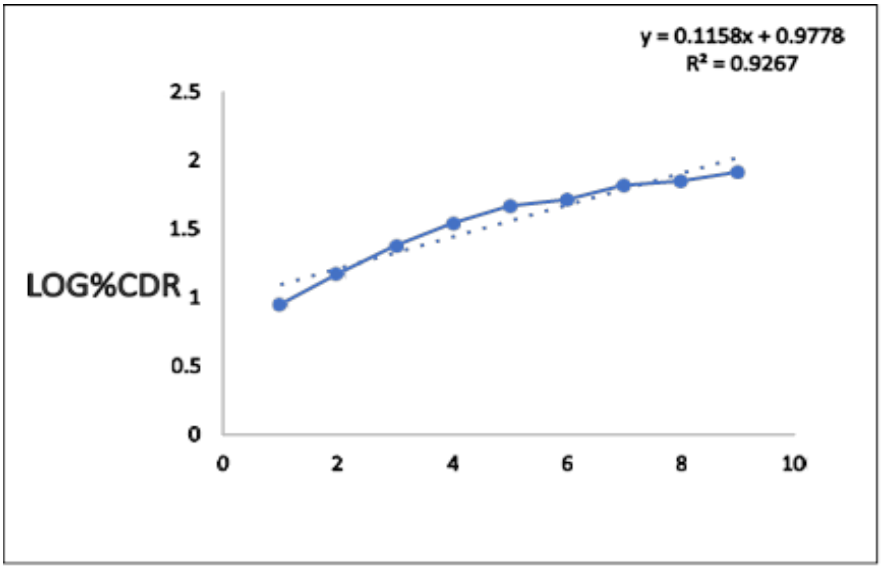

Fig. S19 — First-order release profile of microemulgel G1 showing diffusion-dominant behavior.

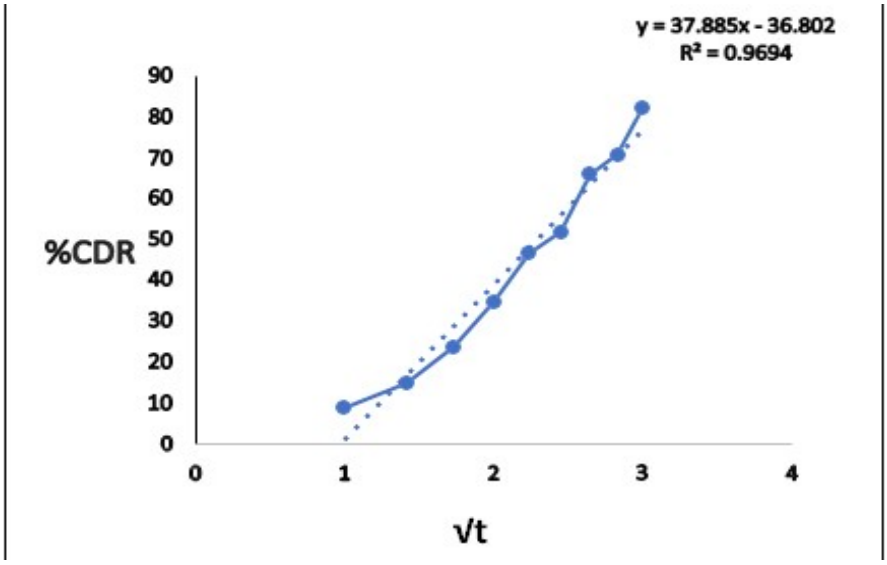

Fig. S20 — Higuchi model plot of G1 microemulgel indicating matrix-type diffusion.

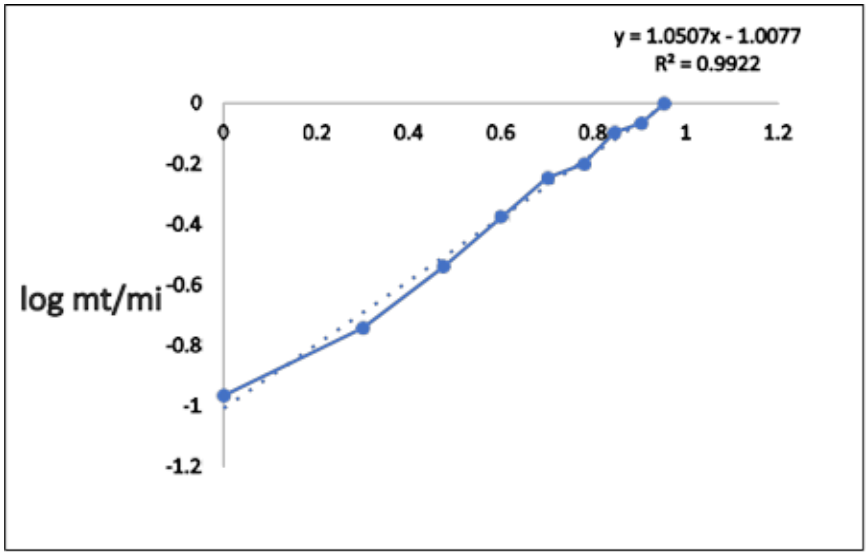

Fig. S21 — Korsmeyer–Peppas model of drug release from microemulgel G1 with R^2 = 0.9922 suggesting anomalous transport.